String-theory-based predictions for nonhydrodynamic collective modes in strongly interacting Fermi gases

Bantilan, H; Brewer, JT; Ishii, T; Lewis, WE; Romatschke, P

String-theory-based predictions for nonhydrodynamic collective modes in strongly interacting Fermi gases

H. Bantilan,[1,2,3] J. T. Brewer,[4] T. Ishii,[5,6] W. E. Lewis,[5] and P. Romatschke[5,6]

[1]*School of Mathematical Sciences, Queen Mary University of London, E1 4NS, United Kingdom*

[2]*Centre for Research in String Theory, School of Physics and Astronomy, Queen Mary University of London, E1 4NS, United Kingdom*

[3]*DAMTP, University of Cambridge, CB3 0WA, United Kingdom*

[4]*Center for Theoretical Physics, MIT, Cambridge, Massachusetts 02139, USA*

[5]*Department of Physics, 390 UCB, University of Colorado at Boulder, Boulder, Colorado 80309, USA*

[6]*Center for Theory of Quantum Matter, University of Colorado, Boulder, Colorado 80309, USA*

(Received 16 June 2016; revised manuscript received 4 August 2016; published 19 September 2016)

Very different strongly interacting quantum systems such as Fermi gases, quark-gluon plasmas formed in high-energy ion collisions, and black holes studied theoretically in string theory are known to exhibit quantitatively similar damping of hydrodynamic modes. It is not known if such similarities extend beyond the hydrodynamic limit. Do nonhydrodynamic collective modes in Fermi gases with strong interactions also match those from string theory calculations? In order to answer this question, we use calculations based on string theory to make predictions for modes outside the hydrodynamic regime in trapped Fermi gases. These predictions are amenable to direct testing with current state-of-the-art cold atom experiments.

DOI: 10.1103/PhysRevA.94.033621

I. INTRODUCTION

Traditional descriptions of quantum matter rely heavily on approaches formulated in terms of particlelike constituents, ranging from ordinary electrons, nuclei, and photons to fermions in Fermi liquids and phonons in superfluids. These particle-based descriptions are and have been extremely successful and provide the backbone of modern physics' ability to describe nature.

Recently, however, it has become clear that there is an ever growing class of strongly interacting systems where particle-based descriptions simply do not work, such as in the mysterious normal state of high-temperature superconductors, fractional quantum Hall effect, extremely hot quark-gluon plasmas, and ultracold quantum gases. Precision experiments in the past decade suggest that despite the fact that quark-gluon plasmas and ultracold quantum gases differ by no less than 18 orders of magnitude in temperature, their ability to flow around obstacles is very similar. This notion can be quantified by comparing the ratio of shear viscosity η to the entropy density s for both normal fluids, finding $\eta k_B/\hbar s \simeq 0.2 \pm 0.1$ for the quark-gluon plasma [1] and $\eta k_B/\hbar s \simeq 0.2 - 0.4 \pm 0.1$ for ultracold quantum gases [2], where $\hbar$ is Planck's constant divided by 2π and k_B is Boltzmann's constant. It should be noted that in both these systems the precise determination of $\eta k_B/\hbar s$ is still an ongoing effort and requires further experimental and theoretical studies [3–7]. Nevertheless, it seems to be an established fact that the quark gluon plasma and ultracold quantum gases have (minimum) values of $\eta k_B/\hbar s$ which differ only by a factor of a few at most.

Unlike ordinary liquids which have particlelike constituents, long-lived particles do not seem to exist for strongly interacting quantum liquids such as hot quark-gluon plasmas and ultracold quantum gases. This breakdown of traditional particle-based methods motivates the search for new, non-particle-based descriptions of strongly interacting quantum matter. One recently developed theoretical tool for strongly interacting systems that does not rely on any particle-based description is the conjectured duality between classical black holes and strongly interacting quantum field theories originating in string theory [8]. Within this framework, it is possible to calculate the friction coefficient η/s for a strongly interacting quantum liquid. One obtains $\eta k_B/\hbar s = 1/4\pi \simeq 0.08$, which is close to the experimentally determined values for both hot quark-gluon plasmas and ultracold quantum gases [9].

The fact that very different systems such as hot quark-gluon plasmas, ultracold quantum gases, and black holes in low-energy string theory have quantitatively similar values of η/s has led to the conjecture that transport properties in strongly interacting quantum liquids are approximately universal [10]. In cold Fermi gases, the presence of a quantum critical point at zero density and temperature also gives rise to universal scaling properties of thermodynamic and transport quantities; cf. Refs. [11,12]. This quantum critical point universality is different from the universality discussed above, which is thought to originate from the strongly coupled nature of different systems. Indeed, neither quark-gluon plasmas nor the black hole considered here are close to a quantum critical point. Universality would imply that the transport properties of a given strongly interacting liquid are matched quantitatively by any other realization of a strongly interacting liquid as long as basic symmetry requirements are fulfilled, even if the liquids themselves have very different constituents, temperatures, or densities. In the case at hand, exact universality cannot be expected, as is already evident from the somewhat different values of η/s for quark-gluon plasmas, ultracold quantum gases, and black holes. However, studying approximate symmetries in physics has had enormous successes in the past, as is evident in the cases of chiral symmetry of the strong force and parity symmetry of the weak force to name two prominent examples. Thus it may nevertheless be useful to consider the possibility of approximate universality concerning the transport properties of different strongly interacting quantum liquids.

The aim of the present work is to test approximate transport universality of strongly interacting quantum fluids by making experimentally testable predictions. Examining the case of

black holes as one example of strongly interacting quantum fluids, one finds that a robust transport feature of black holes is the existence of so-called nonhydrodynamic quasinormal modes, which characterize the ring-down of the black hole after some perturbation occurred (see Ref. [13] for an in-depth review of the physics of quasinormal modes of black holes). If transport properties of strongly interacting fluids are approximately universal, we expect these nonhydrodynamic modes to be realized in ultracold quantum gases. In the remainder of this article, we assume that a commonly studied experimental setup for ultracold Fermi gases admits a gravity-dual approximation in terms of a black hole. We then proceed to make quantitative predictions for the frequencies and damping rates of nonhydrodynamic modes based on this model. These predictions are within the reach of current state-of-the-art experiments, and can be checked by higher-precision experimental data. A detection of nonhydrodynamic modes in ultracold Fermi gases would support the conjectured approximate universality of transport properties among strongly interacting quantum fluids

The remainder of the work is organized as follows. In Sec. II, we review the experimental setup to study collective oscillations in ultracold Fermi gases. In Sec. III, the theoretical calculations of the nonhydrodynamic modes are described, including a summary of assumptions used to convert these calculations to experimentally accessible predictions. Section IV contains our results and we conclude in Sec. V.

II. COLLECTIVE OSCILLATIONS IN ULTRACOLD FERMI GASES

Experiments on ultracold Fermi gases are particularly suited for testing the strong-coupling transport universality hypothesis because they offer the possibility of studying systems in two and three spatial dimensions, with tunable interaction strength, while offering direct real-time information about the density profile and correlations of the gas. The limit of strong interactions is achieved experimentally by tuning a bias magnetic field until the gas experiences a broad Feshbach resonance at which the s-wave scattering length a diverges (unitary regime). Placing the gas of fermionic atoms in a deep optical trap with trapping frequencies $\omega_x,\omega_y,\omega_z$ in the x, y, and z directions then allows experimentalists to routinely measure time-resolved oscillations of the radii of the gas cloud's shape, from which the frequency and damping of the underlying collective modes can be extracted [14–16]. The time evolution of the cloud's shape in two dimensions can be studied experimentally by making the trapping frequency ω_z much larger than both ω_x,ω_y, so that the gas cloud is extremely compressed in the z direction, and for $\omega_x \simeq \omega_y$ the cloud shape resembles that of a pancake. By contrast, if ω_z is much smaller than both ω_x,ω_y the cloud shape resembles that of a cigar. Oscillations of the shape of the cigar in the x-y plane will be referred to as three-dimensional dynamics in the following.

Two independent cloud shape oscillation modes which will be discussed in the following are sketched in Fig. 1. One distinguishes between a radial quadrupole mode, corresponding to elliptic deformations without volume change, and a breathing mode. The amplitude $Q(t)$ for the quadrupole mode can be accessed experimentally by measuring the difference in the width of the main axes, while the amplitude $B(t)$ for

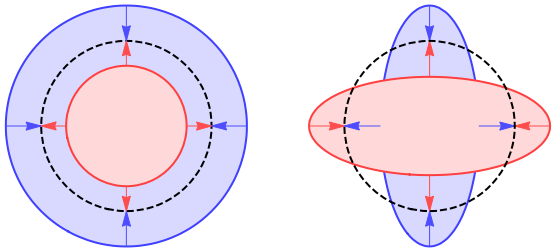

FIG. 1. Sketch of shape oscillations of an atomic gas cloud in the x-y plane: breathing mode (left) and quadrupole mode (right). The breathing mode changes the overall cloud volume, while the quadrupole mode corresponds to a surface deformation without volume change. The cloud's equilibrium configuration is indicated by the dashed circle.

the breathing mode is obtained by summing the widths. A simple approximation to describing the time evolution of the cloud's shape oscillations for a strongly interacting Fermi gas is provided by the equations of hydrodynamics, more precisely the Navier-Stokes equations. (We will limit our discussion to temperatures above the superfluid phase transition where single-fluid hydrodynamics is applicable). For a harmonic trapping potential and small oscillation amplitudes one finds analytic solutions to $B(t), Q(t)$ that are in the form of damped harmonic oscillations [17,18]:

$$B(t) \propto \cos(\omega_B t)e^{-\Gamma_B t}, \quad Q(t) \propto \cos(\omega_Q t)e^{-\Gamma_Q t}. \quad (1)$$

The frequencies ω and damping rates Γ for these hydrodynamic modes differs between breathing and quadrupole mode. Specifically, one finds $\omega_Q = \sqrt{2}\,\omega_\perp$, $\Gamma_Q = \eta\,\omega_\perp^2/P$ for the hydrodynamic quadrupole mode in both $d = 2$ and $d = 3$ dimensions. In the case of the breathing mode, $\omega_B = \sqrt{10/3}\,\omega_\perp$, $\Gamma_B = \eta\,\omega_\perp^2/3P$ for the $d = 3$ breathing mode [10,15,19]. (The breathing mode in two dimensions is undamped and will not be considered in the following.) In expressions above, P denotes the local equilibrium pressure of the strongly interacting Fermi gas, $\omega_\perp \equiv \sqrt{\omega_x\omega_y}$ is the average trap frequency in the x-y plane, and a constant ratio η/P has been assumed in order to derive these analytic results.

III. BLACK HOLE DUAL CALCULATION FOR NONHYDRODYNAMIC FREQUENCIES AND DAMPING RATES

The hydrodynamic modes should be contrasted with the corresponding collective modes expected from a string-theory-based approach. String-theory-based calculations employ so-called black hole duals to calculate properties of strongly interacting matter. In addition to hydrodynamic modes, black holes have an infinite number of nonhydrodynamic collective excitations (quasinormal modes), which are similar to the ring-down modes of a glass struck (lightly) with a fork. As a working definition, nonhydrodynamic modes are modes that do not arise when studying solutions of the Navier-Stokes equations. Despite recent progress [20–22], no exact black hole dual description is known for a strongly interacting Fermi gas. However, one may attempt to use known duals that at least describe bulk features of cold atomic systems in d (spatial) dimensions. In order to describe a nonrelativistic strongly

interacting liquid, we select a black hole dual that correctly reproduces the equation of state (the relation between pressure P to energy density ϵ) of a strongly interacting Fermi gas. Lifshitz black holes have a scaling parameter z that enters the equation of state as $\epsilon z = Pd$ [23]. Since a strongly interacting Fermi gas in d dimension has $\epsilon = Pd/2$ we choose $z = 2$.

For Lifshitz black holes at finite temperature T and zero chemical potential, which are the ones considered in the following, the ratio of shear viscosity to entropy density is known to be $\eta k_B/\hbar s = 1/4\pi$ [24]. In addition, the ring-down spectrum is straightforward to evaluate using a probe scalar with operator dimension Δ. The operator dimension controls the type of perturbation considered. For instance, for density perturbations (fermionic bilinears), the operator dimension would be $\Delta = d$, while for energy density perturbations (fermionic bilinears with a gradient), $\Delta = d + 1$. While it is not known exactly which operator dimension corresponds to the case of density perturbations in the strongly interacting Fermi gas, a reasonable assumption is that Δ is bounded by the cases $\Delta = d$ and $\Delta = d + 1$, so final results including systematic error estimates will be based on the mean and difference from these two choices. To be specific, we compute the quasinormal modes of a scalar field propagating in a fixed Lifshitz black brane background, using the setup described in [25].

In the case of $d = z$, analytic expressions for the ring-down frequencies and damping rates were found in Ref. [25], and we use these for $d = 2$

$$\omega_n^{(d=2)} = 0, \quad \Gamma_n^{(d=2)} = \left(n - 1 + \frac{\Delta}{2z}\right) 4\pi k_B T/\hbar, \quad n \geqslant 1. \tag{2}$$

For $d = 3$, we determine the corresponding values numerically following the general approach outlined in [26], and collect the results in Table I.

The results in Table I all scale as $4\pi T$ for a liquid of temperature T, vanishing chemical potential, and shear viscosity over entropy ratio of $\eta/s = \hbar/4\pi k_B$. This situation differs from the case of real Fermi gases because no exact dual to real Fermi gases is known. Real Fermi gases have sizable chemical potential, small temperature, and shear viscosity over entropy ratios different from $\eta/s = \hbar/4\pi k_B$. In order to connect the string-theory-based calculations to real Fermi gases, guidance from kinetic theory is employed. In kinetic theory, one encounters a single nonhydrodynamic mode with a damping rate $\Gamma_1 = 1/\tau_R$ where the relaxation time τ_R is known to obey $\tau_R \propto \eta/P$ in the hydrodynamic limit [10]. The results from Table I can be brought into this form under the assumption that $4\pi k_B T/\hbar \to sT/\eta$, which is trivially correct for the employed black hole dual. Using furthermore the thermodynamic identity $sT = (\epsilon + P)$ for a fluid with finite temperature and zero chemical potential, it is proposed that the replacement

$$4\pi k_B T/\hbar \to (\epsilon + P)/\eta \tag{3}$$

in the results for the nonhydrodynamic frequencies and damping rates of Table I can be used to connect the black hole dual calculations to real Fermi gases for strong interactions. Once this replacement has been performed, all explicit reference to temperature and chemical potential have been replaced by energy density ϵ and pressure P, which can be applied to a cold strongly interacting Fermi gas with equation of state $\epsilon = Pd/2$ and different values of shear viscosity.

Finally, the above calculations are for the case of an untrapped Fermi gas, rather than a Fermi gas in an optical trap which is studied in most experimental setups. To relate the above untrapped results to the case of a trapping potential with average trapping frequency $\omega_\perp$, again guidance from kinetic theory is used. In kinetic theory, hydrodynamic mode oscillations change qualitatively between a free system and a system placed in a trap, but the nonhydrodynamic modes do not change at all (cf. Ref. [10]). Based on this observation, the nonhydrodynamic mode frequencies and damping rates from the black hole dual calculation of an untrapped system above are directly applied to the case of a trapped Fermi gas.

TABLE I. Numerical results for frequencies and damping rates for ring-down frequencies for $d = 3$ and two choices of Δ.

	$\Delta = 3$		$\Delta = 4$	
n	$\omega_n\hbar/(4\pi k_B T)$	$\Gamma_n\hbar/(4\pi k_B T)$	$\omega_n\hbar/(4\pi k_B T)$	$\Gamma_n\hbar/(4\pi k_B T)$
1	0.2812	0.5282	0.3560	0.7540
2	0.5776	1.437	0.6507	1.663
3	0.8714	2.342	0.9446	2.568
4	1.165	3.246	1.239	3.472

Summary of assumptions

In making predictions for the properties of nonhydrodynamic modes in trapped unitary Fermi gases several assumptions have been made, which are summarized below.

(i) Black holes in asymptotic Lifshitz spaces have been assumed to describe the bulk features of a strongly interacting Fermi gas.

(ii) A probe scalar with dimension $\Delta \simeq d + \frac{1}{2}$ has been assumed to approximately describe density perturbations in the strongly interacting Fermi gas.

(iii) It has been assumed that a strongly interacting Fermi gas at nonzero density and $\frac{\eta k_B}{s\hbar} \neq \frac{1}{4\pi}$ is well approximated by the calculation for a Lifshitz black hole done at zero density and $\frac{\eta k_B}{s\hbar} = \frac{1}{4\pi}$ when performing the replacement (3).

(iv) It has been assumed that the frequencies and damping rates of nonhydrodynamic modes do not differ between the untrapped and trapped Fermi gas.

All of these assumptions can in practice be tested and in most cases lifted by performing more general calculations. However, we leave these more demanding calculations for future work.

IV. RESULTS

Let us consider density perturbations in a trapped, unitary Fermi gas. Besides the familiar hydrodynamic component, the dual black hole calculation implies that there are an infinite number of nonhydrodynamic modes with relative amplitudes α_n. A single nonhydrodynamic mode also is present in kinetic theory [10]; however, kinetic theory is a

TABLE II. Numerical values for the frequencies and damping rates of the first $n \leqslant 4$ nonhydrodynamic modes in $d = 2$ and $d = 3$ dimensions, obtained from a string-theory-based calculation. Results are expressed in terms of the ratio of pressure P to shear viscosity η. Note that P/η can be reexpressed in terms of the damping rates Γ_Q, Γ_B of the hydrodynamic quadrupole and breathing modes for a strongly interacting Fermi gas in a trap.

	$d = 2$		$d = 3$	
n	$\omega_n \times \eta/P$	$\Gamma_n \times \eta/P$	$\omega_n \times \eta/P$	$\Gamma_n \times \eta/P$
1	0	1.25(25)	0.8(1)	1.6(3)
2	0	3.25(25)	1.5(1)	3.9(3)
3	0	5.25(25)	2.3(1)	6.1(3)
4	0	7.25(25)	3.0(1)	8.4(3)

weak-coupling, particle-based description not quantitatively applicable to strongly interacting Fermi gases, so it is unclear how to interpret the kinetic theory result. If black hole duals can be used to describe real unitary Fermi gases then this implies that density perturbations give rise to generalized breathing and quadrupole modes of the form

$$H(t) = \alpha_H \cos(\omega_H t + \phi_H) e^{-\Gamma_H t} + \sum_{n=1}^{\infty} \alpha_n \cos(\omega_n t + \phi_n) e^{-\Gamma_n t}, \quad (4)$$

where $H = B, Q$ depending on the shape oscillation considered, and possible phase shifts ϕ_H, ϕ_n have been allowed.

As outlined in Sec. III, the frequencies ω_n and damping rates Γ_n of the nonhydrodynamic modes can be calculated with the black hole dual for both $d = 2$ and $d = 3$ dimensions. The results from Sec. III have been condensed into experimentally accessible quantities for both $d = 2,3$ shown in Table II. Note that, for two dimensions, the result can be obtained analytically for all n, and one finds $\omega_n = 0$ and $\Gamma_n = (2n - 3/4 \pm 1/4) P/\eta$.

Note that, unlike the hydrodynamic component, the frequencies ω_n and damping rates Γ_n of the nonhydrodynamic modes turn out to be independent of the cloud's average trapping frequency $\omega_\perp$. While the spatial oscillation structure of the nonhydrodynamic modes is exactly equal to those of the well-known hydrodynamic breathing and quadrupole modes, their respective time-dependent signature is quite different. Inspecting Table II it becomes apparent that the nonhydrodynamic modes are excitations with damping rates larger than the oscillation frequency in all cases. (For two dimensions, the analytic result implies that the excitations are purely damped, corresponding to an exponentially decreasing evolution without harmonic oscillations). The different time dependence offers an experimental handle to distinguish these nonhydrodynamic modes from well-studied hydrodynamic oscillations.

In order to facilitate experimental detection of these nonhydrodynamic collective modes, results from Table II have been converted into predictions in Fig. 2 for damping rates expressed in terms of the experimentally measured quantities. For this conversion, the relation between the hydrodynamic damping rates and η/P discussed in Sec. II has been used to reexpress the predicted nonhydrodynamic damping rates from Table II in terms of the damping rates Γ_Q, Γ_B for the hydrodynamic modes [28]. The damping rates Γ_Q, Γ_B themselves have been measured experimentally in two and three dimensions, respectively [14–16]. For example, $\Gamma_1 = 1.25(25)\frac{P}{\eta}$ for the $d = 2$ quadrupole mode from Table II becomes $\Gamma_1 = 1.25(25)\Gamma_Q^{-1}\omega_\perp^2$ which becomes $\Gamma_1 \simeq 4.17(83)\omega_\perp$ when using the experimentally determined value of $\Gamma_Q \simeq 0.30\omega_\perp$ from Ref. [16] at $\ln(k_F a) \simeq 1.04$. In Fig. 2, predictions for nonhydrodynamic mode damping rates $\Gamma_n/\omega_\perp$ are shown in the case of the two-dimensional quadrupole mode and the three-dimensional breathing mode, given different choices of temperature and atom interaction strength. For reference, also shown in Fig. 2 are the only published constraints on the two-dimensional quadrupole mode damping rate Γ_1 extracted from experimental data [10].

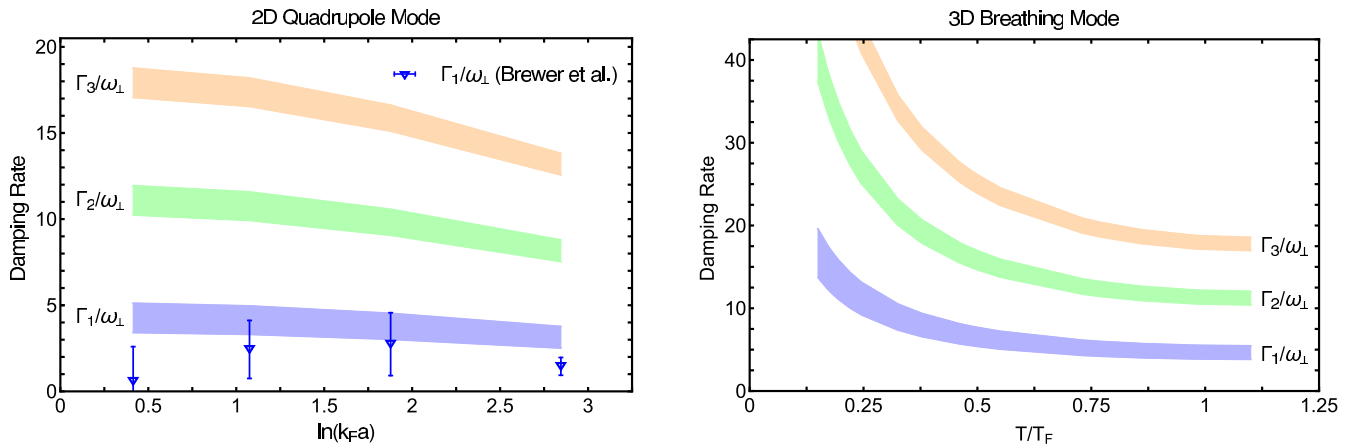

FIG. 2. Predicted nonhydrodynamic mode damping rates $\Gamma_n/\omega_\perp$ (bands). Left: two-dimensional quadrupole mode as a function of interaction strength $\ln(k_F a)$, where a is the two-dimensional s-wave scattering length and k_F is the Fermi momentum [27] related to the density n at the cloud's center as $n = k_F^2/2\pi$. Also shown is the damping rate Γ_1 of the first nonhydrodynamic mode extracted from experimental data [10]. Right: three-dimensional breathing mode as a function of cloud's temperature in units of the Fermi temperature $T_F = (3N\omega_x\omega_y\omega_z)^{1/3}\hbar/k_B$, where $N \simeq 5 \times 10^5$ is the number of atoms in the three-dimensional optical trap.

In Ref. [10], existing experimental data [16] on the quadrupole mode in a two-dimensional trapped Fermi gas had been reanalyzed using a two-component form (4). Given the time resolution and number of data sets obtained in the experiment, the reanalysis performed in Ref. [10] found that information about a predicted second component could be extracted from the data, albeit with low statistical significance. This can be understood through the fact that the measured amplitude $Q(t)$ is most sensitive to the predicted nonhydrodynamic component in Eq. (4) at early times, thus requiring a high time-sampling frequency. In contrast, the main aim in Ref. [16] had been extraction of the hydrodynamic component which requires long-time information. As a consequence, the time-sampling rate chosen in Ref. [16] is not optimal to extract early-time information with high statistical significance. It is likely that the statistical significance of the nonhydrodynamic component could be vastly improved if the experiment in Ref. [16] could be repeated to yield 100 data sets with time resolution increased by a factor of 20. Absent newer experimental data, it is nevertheless interesting to note that the experimental constraints on Γ_1 obtained in Ref. [10] are broadly consistent with the present predictions.

It is also possible to estimate the amplitude ratio α_1/α_H of the first nonhydrodynamic mode relative to the amplitude of the usual hydrodynamic mode when assuming that standard experimental procedures are used to excite quadrupole and breathing mode oscillations [14–16]. Assuming random phase shifts ϕ_H,ϕ_1 for individual hydrodynamic and nonhydrodynamic components, one finds $|\frac{\alpha_1}{\alpha_H}| \simeq (\omega_H + \Gamma_H)/(\omega_1 + \Gamma_1)$. This result would imply typical amplitude ratios of $|\frac{\alpha_1}{\alpha_H}| \simeq$ 40% for the two-dimensional quadrupole mode and $|\frac{\alpha_1}{\alpha_H}| \simeq$ 20% for the three-dimensional breathing mode. This estimate places the predicted first nonhydrodynamic mode well within the experimental detection capabilities of present state-of-the-art experiments in both two and three dimensions.

V. SUMMARY AND CONCLUSIONS

In this work, strongcoupling calculations based on string theory have been used to make quantitative predictions for the existence and properties of nonhydrodynamic modes in strongly interacting Fermi gases. The temporal signatures, frequencies, and damping rates as well as amplitude of the first nonhydrodynamic mode relative to the well-measured hydrodynamic mode have been predicted for both two and three spatial dimensions. These predictions should be well within the experimental testing capabilities for current state-of-the-art experiments.

Indeed, in Sec. IV it was found that experimental constraints on the nonhydrodynamic mode damping rate Γ_1 in the two-dimensional case are consistent with the present string-theory-based prediction [10]. However, given the large error bars and weak statistical significance of Γ_1 in the analyzed data, this is not sufficient to confirm our present predictions. New, high-precision experimental data would be required to confirm (or rule out) the presence of these nonhydrodynamic modes, and thus provide a first stringent test of strong-coupling transport universality.

ACKNOWLEDGMENTS

This work was supported in part by the Department of Energy, DOE Grant No. DE-SC0008132, Contract No. DE-SC0011090, and European Research Council Starting Grant No. NewNGR-639022. We would like to thank T. Enss, U. Romatschke, J. Thomas, T. Schäfer, and W. van der Schee for fruitful discussions on this topic.

[1] C. Gale, S. Jeon, B. Schenke, P. Tribedy, and R. Venugopalan, Event-by-Event Anisotropic Flow in Heavy-Ion Collisions from Combined Yang-Mills and Viscous Fluid Dynamics, Phys. Rev. Lett. **110**, 012302 (2013).

[2] C. Cao, E. Elliott, J. Joseph, H. Wu, J. Petricka, T. Schäfer, and J. E. Thomas, Universal quantum viscosity in a unitary Fermi gas, Science **331**, 58 (2011).

[3] G. M. Bruun and H. Smith, Shear viscosity and damping for a Fermi gas in the unitarity limit, Phys. Rev. A **75**, 043612 (2007).

[4] T. Enss, R. Haussmann, and W. Zwerger, Viscosity and scale invariance in the unitary Fermi gas, Ann. Phys. (NY) **326**, 770 (2011).

[5] G. Wlazłowski, P. Magierski, and J. E. Drut, Shear Viscosity of a Unitary Fermi Gas, Phys. Rev. Lett. **109**, 020406 (2012).

[6] J. A. Joseph, E. Elliott, and J. E. Thomas, Shear Viscosity of a Unitary Fermi Gas Near the Superfluid Phase Transition, Phys. Rev. Lett. **115**, 020401 (2015).

[7] M. Bluhm and T. Schfer, Dissipative fluid dynamics for the dilute Fermi gas at unitarity: Anisotropic fluid dynamics, Phys. Rev. A **92**, 043602 (2015).

[8] J. M. Maldacena, The large N limit of superconformal field theories and supergravity, Int. J. Theor. Phys. **38**, 1113 (1999) [The Large N limit of superconformal field theories and supergravity, Adv. Theor. Math. Phys. **2**, 231 (1998)].

[9] G. Policastro, D. T. Son, and A. O. Starinets, The Shear Viscosity of Strongly Coupled N = 4 Supersymmetric Yang-Mills Plasma, Phys. Rev. Lett. **87**, 081601 (2001).

[10] J. Brewer and P. Romatschke, Nonhydrodynamic Transport in Trapped Unitary Fermi Gases, Phys. Rev. Lett. **115**, 190404 (2015).

[11] P. Nikolic and S. Sachdev, Renormalization-group fixed points, universal phase diagram, and $1/N$ expansion for quantum liquids with interactions near the unitarity limit, Phys. Rev. A **75**, 033608 (2007).

[12] T. Enss, Quantum critical transport in the unitary Fermi gas, Phys. Rev. A **86**, 013616 (2012).

[13] E. Berti, V. Cardoso, and A. O. Starinets, Quasinormal modes of black holes and black branes, Class. Quantum Grav. **26**, 163001 (2009).

[14] J. Kinast, A. Turlapov, and J. E. Thomas, Damping of a Unitary Fermi Gas, Phys. Rev. Lett. **94**, 170404 (2005).

[15] S. Riedl, E. R. Sánchez Guajardo, C. Kohstall, A. Altmeyer, M. J. Wright, J. H. Denschlag, R. Grimm, G. M. Bruun, and H. Smith, Collective oscillations of a Fermi gas in the unitarity

limit: Temperature effects and the role of pair correlations, Phys. Rev. A **78**, 053609 (2008).

[16] E. Vogt, M. Feld, B. Frohlich, D. Pertot, M. Koschorreck, and M. Kohl, Scale Invariance and Viscosity of a Two-Dimensional Fermi Gas, Phys. Rev. Lett. **108**, 070404 (2012).

[17] T. Schfer and C. Chafin, Scaling flows and dissipation in the dilute fermi gas at unitarity, Lect. Notes Phys. **836**, 375 (2012).

[18] J. Brewer, M. Mendoza, R. E. Young, and P. Romatschke, Lattice Boltzmann simulations of a strongly interacting two-dimensional Fermi gas, Phys. Rev. A **93**, 013618 (2016).

[19] P. Massignan, G. M. Bruun, and H. Smith, Viscous relaxation and collective oscillations in a trapped Fermi gas near the unitarity limit, Phys. Rev. A **71**, 033607 (2005).

[20] D. T. Son, Toward an AdS/cold atoms correspondence: A geometric realization of the Schrödinger symmetry, Phys. Rev. D **78**, 046003 (2008).

[21] K. Balasubramanian and J. McGreevy, Gravity Duals for Nonrelativistic Conformal Field Theories, Phys. Rev. Lett. **101**, 061601 (2008).

[22] X. Bekaert, E. Meunier, and S. Moroz, Towards a gravity dual of the unitary Fermi gas, Phys. Rev. D **85**, 106001 (2012).

[23] C. Hoyos, B. S. Kim, and Y. Oz, Lifshitz hydrodynamics, JHEP 11 (2013) 145.

[24] M. Taylor, Lifshitz holography, Class. Quantum Grav. **33**, 033001 (2016).

[25] W. Sybesma and S. Vandoren, Lifshitz quasinormal modes and relaxation from holography, JHEP 05 (2015) 021.

[26] A. O. Starinets, Quasinormal modes of near extremal black branes, Phys. Rev. D **66**, 124013 (2002).

[27] Unlike the case of three dimensions, the scattering amplitude in two dimensions depends logarithmically on $k_F a$, which makes $\ln(k_F a)$ a good interaction parameter similar to the role played by $1/(k_F a)$ in three dimensions [29].

[28] Having expressed the nonhydrodynamic mode damping rates in terms of Γ_Q, Γ_B allows predictions for variable (but large) interaction parameter even though the underlying calculation is only strictly valid at infinite interaction strength (see Methods section for details).

[29] I. Bloch, J. Dalibard, and W. Zwerger, Many-body physics with ultracold gases, Rev. Mod. Phys. **80**, 885 (2008).